NASA Contractor Report 3800

Support Structures for Large Infrared Telescopes

John M. Hedgepeth

CONTRACT NAS1-16923
JULY 1984

NASA

NASA Contractor Report 3800

Support Structures for Large Infrared Telescopes

John M. Hedgepeth
Astro Research Corporation
Carpinteria, California

Prepared by Astro Research Corporation
for Lockheed Missiles & Space Company, Inc.,
and for NASA Langley Research Center
under Contract NAS1-16923

National Aeronautics
and Space Administration

**Scientific and Technical
Information Branch**

1984

TABLE OF CONTENTS

LIST OF TABLES AND FIGURES

INTRODUCTION

There is historically a gap between the technologies of optical systems and of radio frequency antennas. The gap is, of course, man made because the electromagnetic spectrum is a continuum. The recent attention of radio frequency users to large apertures and small wavelengths and of optical instrument users to the infrared regime has erased the gap. One of the results is that some of the advanced concepts for large antennas in space become useful for infrared telescopes.

Figure 1 shows various ranges of radio frequencies and sizes that are of interest for future large space antennas. Note that the bulk of requirements involves ratios of diameter to wavelength (D/λ) of less than 10,000. Some of the recent advances motivated by these requirements are discussed in references 1 and 2. Much more precise antennas are required for submillimeter and infrared astronomy as can be seen from the figure. Structural configurations designed to meet this higher accuracy requirement are the subject of this paper.

This report is an enlargement of the information published as reference 3. It contains extensive excerpts from that paper for completeness.

LARGE DEPLOYABLE REFLECTOR FOR SPACE-BASED ASTRONOMY

REQUIREMENTS

An example mission which requires very high accuracy is large-aperture infrared astronomy. The instrument for this scientific mission has been under consideration for several years; it is called the Large Deployable Reflector (LDR). In June, a workshop was held at Monterey, California for both experimenters and technologists to investigate what this instrument should be. The following requirements, which are based on the findings of that workshop, have been selected to guide the baseline design of the antenna structure.

Diameter	20-m primary, 1-m secondary
Focal length	20-m primary, 200-m system
Diffraction-limited wavelength	50-micrometers

Pointing	0.05 arcsec absolute 0.02 arcsec jitter
Slew	<20 degrees/min
Scan	1 degree/min
Orbit	750 km, 28 degrees or polar
Chopping	1 arcmin at 2 Hz
Temperature	150 K primary, 125 K secondary
Reflector segments	2-m size, 1.5-micrometer accuracy

BASELINE CONCEPT

The chosen structural concept for the infrared reflector telescope is shown in Figure 2. This is an off-axis Cassegrainian design with a focal length equal to the aperture diameter (the Monterey workshop recommended an on-axis primary reflector with an F/D = 0.5). The larger focal length enables the off-axis system to have a sufficiently wide field of view. The primary mirror is made up of approximately 120 hexagonal 2-m panels. These reflector panels are assumed to be very accurately shaped and very stable in dimensions. Panels are mounted to the truss backup structure with three-point adjustable attachments, and an active control system is used to position the panels in such a way as to yield the required very accurate surface. The subreflector located at the focus of the primary reflector is mounted to the main reflector by a tripod formed of lattice columns. The scientific package is contained in the main spacecraft represented by the four-sided block at the lower left.

In order to reduce the system noise, the reflecting surfaces need to be kept very cold. This can be accomplished passively by excluding external radiation to the primary mirror. A concept of a thermal shield to exclude this radiation is shown in Figure 3. The shield is assumed to be composed of highly efficient multilayer insulation on all sides, including the lower surface of the primary mirror truss. The subreflector and instrument package are assumed to be located opposite to the Sun at all times. Studies show that a serious problem occurs when the spacecraft is on the Sun-lit side of the Earth. Orienting the spacecraft to avoid the impingement of solar radiation in the cavity involves the capture of a significant amount of infrared Earth

radiation and albedo. Consequently, the interior of the thermal shield on the side away from the Earth is composed of corner reflectors so that radiation entering the cavity will be reflected out again.

DEPLOYMENT CONCEPTS

Various means exist for constructing the LDR in space. One approach is illustrated in Figure 4. In this approach, the structural truss would be deployed, and then the reflector panels would be mounted to that truss. Figure 4 shows the mounting being done by the Shuttle Remote Manipulator System (RMS). Other approaches could use EVA (Extra Vehicular Activity).

Figure 5 illustrates another approach in which each reflector panel would be attached to a packaged module of the structural truss. Each module would then be deployed and assembled to its neighbors to create the entire reflector. Again, this assembly work would be done by remote manipulators or by EVA.

When structural joints are to be made on assembly, their design becomes an important consideration. One possible design is shown in Figure 6. The structural connection is made by means of a drogue and probe arrangement. A mechanical fastener of some sort would lock the joint together. Also shown here is an electrical connector which would enable the proper routing of power and signal leads as necessary.

The assembly tasks in the foregoing concepts are characterized by a large ratio of the distance traveled to the dimensional precision of mating the parts. The concept shown in Figure 7 avoids this disadvantage. All the modules are interconnected so that the hinges in the structure furnish a large amount of control to aid the assembly of the modules. This allows the use of a fairly simple special-purpose assembler mounted to the deployment canister which needs only to perform the final close-proximity attachment operations. This concept, which was developed several years ago, is described more fully in references 3 and 4.

Fundamentally, the interconnected reflector-truss modules are packaged in a canister and caused to deploy one at a time as the canister walks itself around the structure. The example shown in Figure 7 is appropriate to a Shuttle-based experiment.

SEQUENTIAL DEPLOYMENT

The sequential deployment design for the LDR would take the form shown in Figure 8. Here, the primary reflector is packaged in a canister about 10 m long. Each stowed reflector truss module would thus be about 8 cm thick. The lattice columns which support the subreflector would be folded at appropriate knee joints, and the packaged telescope without thermal shield would appear as at the top left of the figure. Ample room exists in the Shuttle bay for stowage. The sequence of deployment would be first to put the subreflector into its proper position by releasing appropriate knee hinges. Then the primary reflector canister would construct that portion of the primary reflector until a corner is reached. At that time, the lattice tripod would be further unfolded to reach that corner, the manipulator on the canister being available to help in making the structural joint properly. The canister would then proceed to the other tripod corner with a similar subsequent deployment of the tripod on that side. The remainder of the primary reflector would then be constructed.

Note that no work has yet been done to develop a means to package and deploy the thermal shield. It is expected that it is possible to accomplish this together with the reflector in a single Shuttle payload. One possibility would be to package and deploy the shield separately, perhaps with the aid of EVA.

THERMAL CONTROL

Thermal control is a primary design requirement for the LDR reflector structure. In order to minimize thermal background noise, the primary reflector needs to be maintained at 150 K or colder with no more than 1-K variation across the surface. In order to obtain the required surface accuracy, the supporting structure must be very nearly isothermal with gradients below 1 K. These requirements must be met in low Earth orbit where reflected and emitted Earth radiation, as well as direct solar radiation, levels are high.

The thermal control system has been previously shown in Figure 3. The estimated maximum heating rates of the structure are shown in Figure 9 for an attitude where Earth radiation illuminates the interior walls covered by corner reflectors but does not directly illuminate the reflector. The Earth

radiation impinging on the side wall and entering the top of the shield has been estimated from data in reference 5 for a 750-km altitude. The major contribution to the heating comes from albedo radiation absorbed during the two reflections in the corner reflector. It has also been assumed that some albedo radiation is diffusely reflected towards the reflector. Heat leaks of 1 to 4 W/m^2 through the multilayer insulation have been assumed depending on the incident radiation intensity.

The total of these heat loads to finally be absorbed by the reflector is estimated at 3 W/m^2, including the heat leak through the lower surface. Since the heat load drops nearly to zero at the other extreme of the orbit, the average heating is estimated at 1.5 W/m^2 which corresponds to an equilibrium temperature near 150 K.

The insulation comprising the thermal shield must exhibit very high performance. The heat leaking through a multilayer insulation having n layers is approximately

$$q = \frac{2\Phi\epsilon}{n + 1} \tag{1}$$

where Φ is the intensity of the incident radiation, and ϵ is the emissivity. In this equation, the conductive transfer is assumed to be equal to the radiative transfer.

Each layer of insulation consists of a very thin ($\sim$ 3 micrometers) polymeric film with a metallic low-emissivity coating. Conduction is reduced by insulation separators. A mass density of 13 g/m^2 for each layer is reasonable. The mass of the multilayer insulation is estimated to be (for large n)

$$m_I = 0.026 \frac{\Phi\epsilon}{q} \tag{2}$$

where the units are kg/m^2.

A value of $\epsilon = 0.03$ can be achieved by metallizing with gold.

For the Sun-facing side of the thermal shield, the mass density of the multilayer insulation for an allowed leakage of 4 W/m^2 is

$$m_I = 0.26 \text{ kg/m}^2$$

If only 1 W/m^2 is allowed, as is the case on the back surface, the insulation would weigh about 1 kg/m^2. The total weight of insulation would be about 750 kg.

ACTIVE CONTROL OF THE REFLECTOR PANELS

The LDR must use active control to achieve the high degree of accuracy that is required of it. The needed capability of that active control system is dependent on how well the structure itself maintains the precise geometry. Some facts are that:

- Sensing difficulty is directly dependent on the field of view and inversely dependent on the absolute accuracy desired.
- Computation becomes more lengthy as the ratio of largest to smallest quantity increases.
- Actuators are more complicated as the stroke increases relative to the required movement accuracy.

The conclusion is that the expense of active control is dependent on its basic task of improving accuracy. Thus, if 1-micron accuracy is required, for example, a control system which must operate over a range of a centimeter would be considerably more expensive than one whose stroke, and sensor capability, would be less than a millimeter. The question of how accurately the support structure can be constructed is treated in the next section.

An additional element in determining how complex the control system needs to be is the rate at which changes in geometry of the structure would occur. A very low control bandpass could be tolerated if the geometry would vary at a slow rate. Estimates of the influence of changing thermal and loading conditions are given in following sections.

ACCURACY OF TRUSS REFLECTORS AS FABRICATED

Estimates have been made of how accurately truss-type reflector structures can be built for space applications. Because of the difficulty of constructing and measuring large structures in a 1-g environment, the assumption has been made that the structural components will be manufactured to high accuracy and then assembled without further adjustment. The final structure then will exhibit a surface precision which depends on the way in which the individual inaccuracies combine. In reference 6, an estimate is made of this error by assuming that the truss structure has many cells and, therefore, can be approximated by a continuous structure. Recently, another analysis which treats example trusses in a direct fashion by using the Monte Carlo technique has been made by William H. Greene of NASA Langley Research Center. Thus, a specimen structure is assumed to be built up of struts whose lengths scatter randomly about their design value. The distorted geometry is then calculated by finite-element truss analysis. An average of the squared error over the surface of the truss is determined.

The variation of the rms error as a function of the number of rings in the truss structure is shown in Figure 11. The curve with circles is the mean of 100 trials. The extent to which the rms surface error varies from specimen to specimen is indicated by the 1 σ deviation which is shown as the difference between the square and the circle points. Also shown in the figure is the continuum analysis estimate of reference 6. It is seen that the previous work furnishes a reasonable estimate of the mean error, but does not include the important effects of sample-to-sample variation.

Detailed results for a six-ring LDR structure with an offset focal point are shown in Figure 12. The nondimensional average rms for 100 structures is shown to be 0.245. If we include three standard deviations of the mean square, then the average turns out to be 0.385. This worst-case structure exhibits an error of 2-1/2 times that previously predicted by reference 6.

Note that the rms errors are nondimensionalized with respect to the reflector diameter and the rms unit error in the length of the individual truss members σ_ϵ. For the LDR size and for a reasonable value of σ_ϵ, the product $D\sigma_\epsilon$ is about 1 mm. For this case, the aforementioned numbers can then be interpreted as being the physical rms in millimeters.

Also shown in Figure 12 are data for the rms deviations at individual points on the reflector. This deviation is a function of the position of the point on the truss and tends to grow as the boundary of the reflector is reached. Note that the scatterbands show how much variation exists as points around an individual ring are considered. Presumably, taking a multiple of the rms deviation would give a basis for designing the required stroke of the active control system actuators. This information indicates that a stroke of about 3 mm might be required.

The results shown in Figure 12 are summarized in Figure 13. The dotted line shows the wavelengths of radiation that could be handled by the structure if no active control were employed. The improvement of capability for active control systems of various refinement as measured by ratio of accuracy to full-scale stroke is shown by the solid lines. Examination shows that a control-system accuracy of one part in 2000 would be required in order to handle a wavelength of 50 micrometers with reasonable fabrication tolerances.

INFLUENCE OF THERMAL STRAINS ON SURFACE ACCURACY

One of the most important error-causing disturbances in spaceflight is that of thermal straining. Despite the presumed availability of composite materials with very low thermal expansion coefficients, a change in temperature differentials of a few degrees can cause distortions larger than those allowable for the LDR. Fortunately, in order to meet the low-temperature requirement on the primary mirror, the thermal inputs are very carefully managed. The truss struts supporting the secondary reflector are protected from direct radiation, and the primary-reflector truss occupies a nearly constant-temperature space.

Nevertheless, as the orientation of the LDR changes with respect to the Sun and the Earth, there will occur temperature variations and nonuniformities in the structure. The influence of these changes needs to be estimated in order to determine how severe the distortions may be. Attention is concentrated on the primary-reflector truss inasmuch as it presents the most severe engineering problem.

For purposes of analysis, the reflector support truss can be assumed to occupy an approximately spherical annulus bounded by two curved surfaces - the

reflector panels and the back-surface multilayer insulation. The reflector panels are relatively massive with a large thermal inertia. Therefore, the temperature of the reflector surface varies very slowly.

An estimate of the maximum rate of temperature change can be obtained by determining how fast the reflector cools when all thermal input to it is removed. The results of this simple analysis are shown in Figure 10. For example, at the nominal temperature of 150 K, a 10-kg/m^2 panel will cool at only 0.6 K/hour.

The temperature of the inner wall of the back-surface shield can vary more rapidly because of its low thermal inertia. On the other, the amount of variation must necessarily be limited. Otherwise, the heat flow between the two surfaces (and, hence, through the insulated shield) would be unacceptably large. The temperature difference can be evaluated by assuming that all temperatures are close to the nominal temperature T_0. The unit heat flow q between the two surfaces of emissivity ϵ is

$$q = \epsilon\sigma \left(T_2^4 - T_1^4 \right) \tag{3}$$

where the subscripts 1 and 2 refer to the reflector and shield surfaces, respectively. The quantity σ is the Stefan-Boltzmann constant (= 5.67 x 10^{-8} $W/m^2/K^4$).

Linearizing and solving for the temperature difference gives

$$\Delta T = \frac{q}{4\epsilon\sigma T_0^3} \tag{4}$$

where $\Delta T = T_2 - T_1$.

As an example, let

$T_0 = 150$ K

$\varepsilon = 1$

$q = 1\ W/m^2$

Then the temperature difference is

$\Delta T = 1.3$ K

In this and the subsequent calculations, the emissivity is taken to be unity on all interior surfaces for ease of analysis. Good thermal design may entail high reflectivity of one or more surfaces in order to minimize the temperature variations in the truss. The present estimates should therefore be conservative in this sense.

Assume the shield insulation is indeed designed to limit the heat flow to 1 W/m^2 for worst conditions. Then the value ΔT should vary between $\pm$ 1.3 K. The variation of truss temperature will be less than this.

An estimate of the effect of temperature differentials in the truss can be obtained by assuming that the upper surface of the truss (the one close to the reflector panels) is of different temperature than that of the lower surface. The resulting distortion is approximately a change in curvature of the surface of

$$\Delta k = \frac{\alpha_T (T_L - T_U)}{H} \tag{5}$$

where α_T is the thermal expansion coefficient, and H is the depth of the truss. Assume that the position controller for the secondary reflector can correct for rigid-body displacement of the primary reflector but cannot correct for the change in curvature. Then the distortion will result in an rms displacement of the primary reflector of

$$w_{rms} = \frac{\Delta k}{\sqrt{48}} \left(\frac{D}{2}\right)^2 \tag{6}$$

where D is the diameter of the reflector (taken here to be of circular planform). Substituting for Δk yields

$$w_{rms} = 0.0361 \frac{\alpha_T (T_L - T_U) D^2}{H} \tag{7}$$

The temperature differential across the truss is caused by the curvature of the volume and the blockage of radiation from the reflector and heat shield surfaces by intervening truss members. If conduction within the truss is assumed (conservatively) to be zero, then the temperature at a generic point on the truss is dependent on the temperatures and view factors of the surrounding radiative surfaces, including other portions of the truss. For black-body surfaces and small departures from the nominal temperature, the linearized form of the equation governing radiative equilibrium gives the temperature to be

$$T = \Sigma F_i T_i \tag{8}$$

where F_i is the fraction of the total solid angle occupied by the surrounding surface of temperature T_i.

If there were no curvature and no blockage, the surrounding surfaces would consist of only the reflector and the shield each with form factors of 0.5. The temperature of all interior points would therefore be $(T_1 + T_2)/2$.

The effect of the curvature is to decrease the form factor of the reflector surface by an amount depending on the ratio between the distance

between the point and the reflector surface and the radius of curvature of the surface. For a sphere of radius of twice the focal length F, the form factor is

$$f_1\left(\frac{h}{F}\right) = \frac{1}{2}\left[1 - \frac{\sqrt{h/F + (h/F)^2/4}}{1 + (h/F)/2}\right] \tag{9}$$

where h is the distance from the point to the reflector surface.

The amount of blockage can be estimated by multiplying the solidity of one of the truss surfaces by a factor to represent the blockage of the core members of the truss and to correct for the three-dimensional effects. Thus, for example, a point on the lower surface, for which h = H, has a temperature of

$$T_L = \left[f_1\left(\frac{H}{F}\right) - k\,\frac{2\sqrt{3}d}{\ell}\right]T_1 + k\,\frac{2\sqrt{3}d}{\ell}\,T_U + \left[1 - f_1\left(\frac{H}{F}\right)\right]T_2 \tag{10}$$

where k is the blockage correction factor.

Writing a similar equation for the upper surface and solving for the temperature difference gives

$$T_L - T_U = \frac{\frac{1}{2} - f_1\left(\frac{H}{F}\right) + k\,\frac{2\sqrt{3}d}{\ell}}{1 + k\,\frac{2\sqrt{3}d}{\ell}}\,\Delta T \tag{11}$$

For H = 2 m, F = 20 m, ℓ = 2 m, d = 2 cm, and k = 2, the curvature effect is

$$\frac{1}{2} - f_1\left(\frac{H}{F}\right) = 0.152$$

and the blocking effect is

$$k \frac{2\sqrt{3}d}{\ell} = 0.069$$

Thus,

$$T_L - T_U = 0.207\ \Delta T$$

For the worst-case value of ΔT of 1.3 K, the temperature differential across the truss is only 0.25 K. For a readily achievable thermal expansion coefficient of 0.5×10^{-6}/K, the resulting rms distortion is

$$w_{rms} = 0.9\ \mu m$$

which is pleasantly small.

The results of the foregoing analysis are summarized in Figure 14 which gives the limitations on the diameter-to-wavelength ratio for reflectors in which the rms surface error is less than 1/100 of the wavelength. The abscissa is the product of the overall temperature difference within the insulated cavity in which the support truss is located and the thermal expansion coefficient. Curves are shown for various values of H/D. In all cases, values of F/D = 1 and $kd/\ell = 0.02$ were assumed. Incidentally, the influence of those two parameters on the diameter-to-wavelength ratio is small, a factor of two change in either parameter effecting the ratio by less than about 20 percent.

The results show that maintaining the desired precision of the primary reflector for the 20-m baseline configuration requires that $\alpha_T \Delta T$ be less than 5×10^{-7} for a truss depth of 2 m. Meeting this requirement is within the

current state of the art. The conclusion can therefore be drawn that the probability is high that thermal changes will not produce unacceptable distortions in the primary reflector.

INFLUENCE OF ACCELERATIONS ON SURFACE ACCURACY

As is pointed out in reference 1, the primary structural requirement is to provide enough stiffness to maintain the desired dimensional stability despite the loads (albeit small) imposed on the spacecraft. This is particularly true for the present application if the structure is expected to maintain precision passively without depending on the active control system to correct for short-time changes in loading. The intent of this section is to estimate the amount of excitation and to determine approximately the conditions for which the excitation can be handled passively.

ANGULAR ACCELERATIONS

Attention will be concentrated on the various sources of angular acceleration:

(a) Gravity Gradient: From reference 1, the equivalent angular acceleration that causes the same loading as gravity gradient in a 750-km orbit is

$$\ddot{\theta} = 3.5 \ \mu\text{rad/sec}^2$$

(b) Slewing: The slewing velocity of 20 degrees/minute can cause centrifugal accelerations that will cause distortion. An equivalent angular acceleration can be estimated by squaring the rotation rate. This gives

$$\ddot{\theta} = 34 \ \mu\text{rad/sec}^2$$

The transient acceleration can also be estimated by assuming that 1 minute is used to accelerate to full slewing velocity. This yields

$$\ddot{\theta} = 97 \ \mu\text{rad/sec}^2$$

(c) Chopping: The beam chopping is supposed to be performed without reactions. Some residual from this and other sources can be expected, however. If the effect on the pointing accuracy is to be kept less than the jitter budget of 0.02 arcsec, the acceleration at 2 Hz is

$$\ddot{\theta} = 15.3 \ \mu\text{rad/sec}^2$$

The conclusion is that the structure needs to cope with angular accelerations of about 100 μrad/sec^2.

DISTORTIONS

The torque Q that must be applied to the primary reflector through the corners in order to produce an acceleration of $\ddot{\theta}$ is given by

$$Q = \frac{\pi}{64} m_T D^4 \ddot{\theta} \tag{12}$$

where m_T is total mass density of the reflector. It is composed of the mass density of the panels m_P, the insulation m_I, and the structure m_S.

The analysis is given in the Appendix of the rms distortion caused by such a torque applied at the centerline and two symmetrically located points at the rim. The result for the present configuration is

$$\frac{w_{rms}}{D} = 0.0418 \frac{Q}{D_s} \tag{13}$$

where D_s is the equivalent plate stiffness which, for a tetrahedral truss of member length ℓ and depth H, is

$$D_s = \frac{3\sqrt{3}}{8} \frac{\eta EA \ H^2}{\ell} \tag{14}$$

Note that the joint efficiency parameter η is used to account for the reduction in extensional stiffness EA of the truss members due to compliance of the deployable joints.

MEMBER SIZE

Combining the foregoing equations yields an expression for the member size

$$A = 0.00316 \frac{D^4 \ell}{\eta H^2} \frac{m_T \ddot{\theta}/E}{w_{rms}/D} \tag{15}$$

For

$\ddot{\theta} = 100\ \mu rad/sec^2$

$D = 20\ m$

$\ell = H = 2\ m$

$\eta = 0.5$

$E = 124.5\ GN/m^2$

$w_{rms} = 0.5\ \mu m$

The design member cross-sectional area is

$$A/m_T = 1.62 \times 10^{-5}\ m^2/kg/m^3$$

Let the total mass density be 50 kg/m^2, which would consume about 50 percent of the total mass budget for the primary reflector. If the member area is circular and solid, the diameter is 3.2 cm. If lighter panels are available, the member sizes can be smaller. For example, a total mass density

of 20 kg/m^2 would yield a solid strut diameter of 2 cm. For even lighter panels, the choice would be to make the members hollow in order to avoid too slender a strut.

SUPPORT TRUSS MASS

For the tetrahedral truss, the length of members per unit of planform area is

$$\frac{4(\sqrt{3}+1)}{\ell}$$

where the first term includes the surface members and the second the core members for which a value of $H = \ell$ has been assumed. The resulting structural mass density is

$$m_S = \frac{10.93\ k\rho A}{\ell} \tag{16}$$

where k is the joint and fitting mass factor and ρ is the density of the strut material.

Substituting into the previous equations gives

$$\frac{m_S}{m_T} = 0.0345\ \frac{k\rho D^4}{\eta H^2}\ \frac{\ddot{\theta}/E}{w_{rms}/D} \tag{17}$$

For the values used previously and with k = 2 and $\rho = 1520\ kg/m^3$

$$\frac{m_S}{m_T} = 0.270$$

which is a reasonable structural mass fraction.

TRIPOD DESIGN

The three struts supporting the secondary reflector will deform axially due to the angular acceleration. An analysis of the stiffness furnished by this arrangement for F = D gives the coefficient for the deflection due to loading in the least stiff direction (slightly above the horizontal) to be

$$\frac{\Delta}{p} = 4.8 \frac{D}{EA} \tag{18}$$

where A is the area of each of the three longerons in the struts.

For the small member area as obtained for the reflector truss, the value for the 50-kg/m^2 design is

$$\frac{\Delta}{p} = 0.95 \ \mu m/N$$

For the 20-kg/m^2 design, it is

$$\frac{\Delta}{p} = 2.38 \ \mu m/N$$

If the mass of the secondary reflector is 1000 kg, then the inertia force induced by an angular acceleration of 100 μrad/sec^2 at a distance of 20 m is 2 N. The consequent deflection is satisfactorily small in both cases.

VIBRATION FREQUENCIES

The structure that is designed to yield high stiffness will also yield high natural vibration frequencies. While a computer analysis is needed to determine the overall frequencies, some estimates can be made as follows.

Consider first the reflector. Its frequency as a free-free structure can be estimated from the equivalent circular plate as

$$f = \frac{21.0}{2\pi} \sqrt{\frac{D_s}{m_T D^4}} \tag{19}$$

For the values used previously, the frequency is

$$f = 9.6 \text{ Hz}$$

Of course, the fundamental coupled frequency will be smaller than this. On the other hand, it must be higher than that obtained by fixing the dish at the tripod attachments. This latter frequency can be estimated by considering a cantilever beam of length D and the same mass and stiffness properties as those of the truss. This lower-bound frequency is 1.6 Hz.

The vibration frequency of the secondary reflector mounted to the tripod assumed fixed at its base is

$$f = \frac{1}{2\pi} \sqrt{\frac{EA}{4.8\ D\ M_{sec}}} \tag{20}$$

For a secondary reflector mass of M_{sec} 1000 kg, the frequency for the 50-kg/m^2 design is

$$f = 5.16 \text{ Hz}$$

and for the 20-kg/m^2 design

$$f = 3.27 \text{ Hz}$$

The lateral vibration frequencies of the tripod struts are dependent on their cross-sectional size. Let b be the width of each face of the triangular strut. Let k_s be the ratio of total mass of the strut to the mass of its longerons. Then the simply supported vibration frequency is

$$f = \frac{\pi}{2}\sqrt{\frac{Eb^2}{6k_s\rho L^4}} \tag{21}$$

where L is the length of the strut. For b = 0.5 m and L = $\sqrt{500}$ m, the lateral frequency is

$$f = 2.9 \text{ Hz}$$

CONCLUDING REMARKS

The analyses in this report are only a beginning to those which are needed to evaluate the structural potentials and problems associated with the LDR. The results indicate, however, that even so challenging a requirement as the LDR can be dealt with by good structural design. It appears to be possible to provide a very stable support structure that distorts only slightly due to thermal and loading inputs. The active control system therefore can be designed to have a low band pass thereby enabling sufficient time for sensing, computation, and actuation without the necessity of heroics. The implications with regard to program risk and cost are evident.

REFERENCES

1. Hedgepeth, John M.: Critical Requirements for the Design of Large Space Structures. NASA CR-3484, 1981.
2. Hedgepeth, John M.; and Adams, Louis R.: Design Concepts for Large Reflector Antenna Structures. NASA CR-3663, 1983.
3. Hedgepeth, John M.: Design Concepts for Reflector Antenna Structures. Paper No. 383-05. Presented at the SPIE Technical Symposium, 18 and 19 January 1983, Los Angeles, CA. Published in Symposium Proceedings, Vol. 383.

4. Hedgepeth, John M.; and Finley, Laurence A.: Deployable Structures for Millimeter-Wave Antennas. Astro Research Corporation, ARC-TN-1087, 14 April 1980.

5. Finley, Laurence A.: The Geometry of the 37-Tile Microwave Antenna Support Structure. Astro Research Corporation, ARC-TN-1083, 5 March 1980.

6. Brogren, E.W.; Barclay, D.L.; and Straayer, J.W.: Simplified Estimation Thermal Techniques for Large Space Structures. NASA CR-145253, October 1977.

7. Hedgepeth, John M.: Influence of Fabrication Tolerances on the Surface Accuracy of Large Antenna Structures. AIAA Journal, vol. 20, no. 5, May 1982, pp. 680-686.

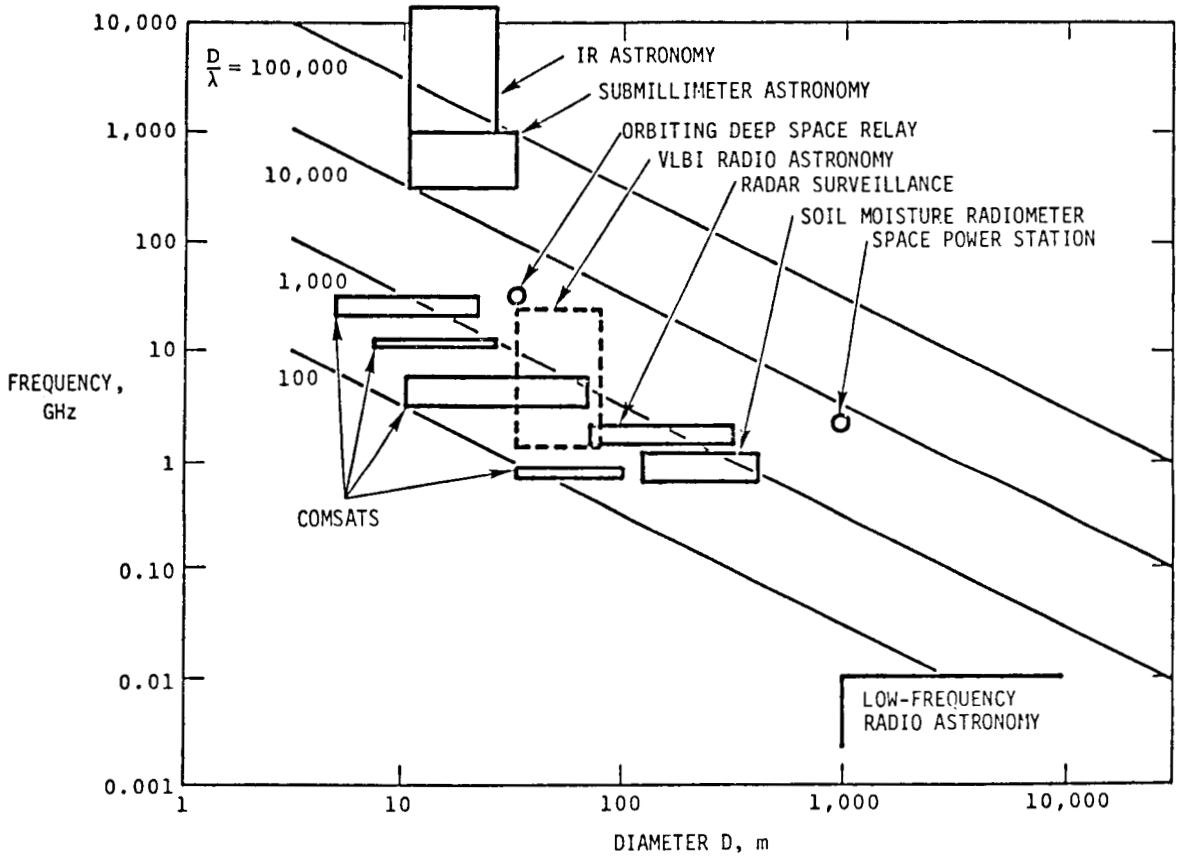

Figure 1. Large space antenna requirements. *034A*

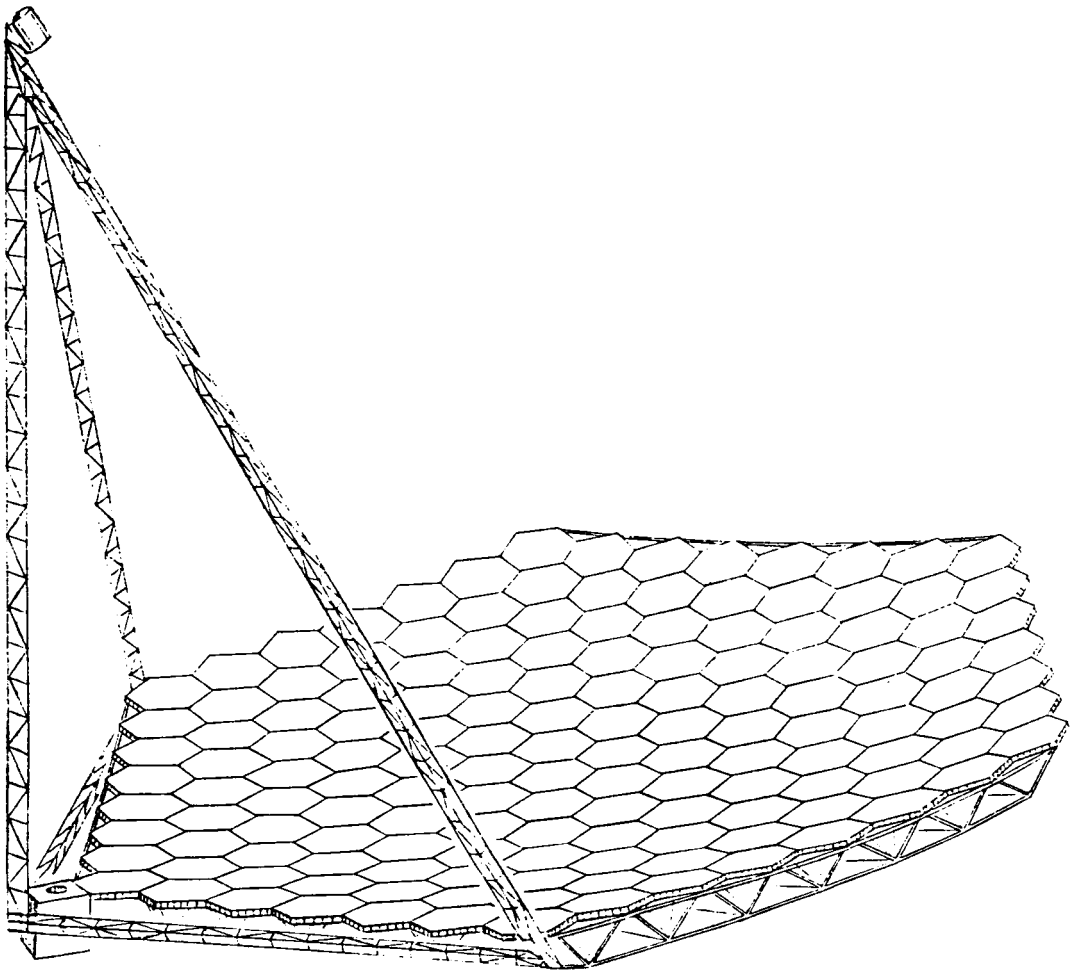

Figure 2. Baseline precision reflector. 035A

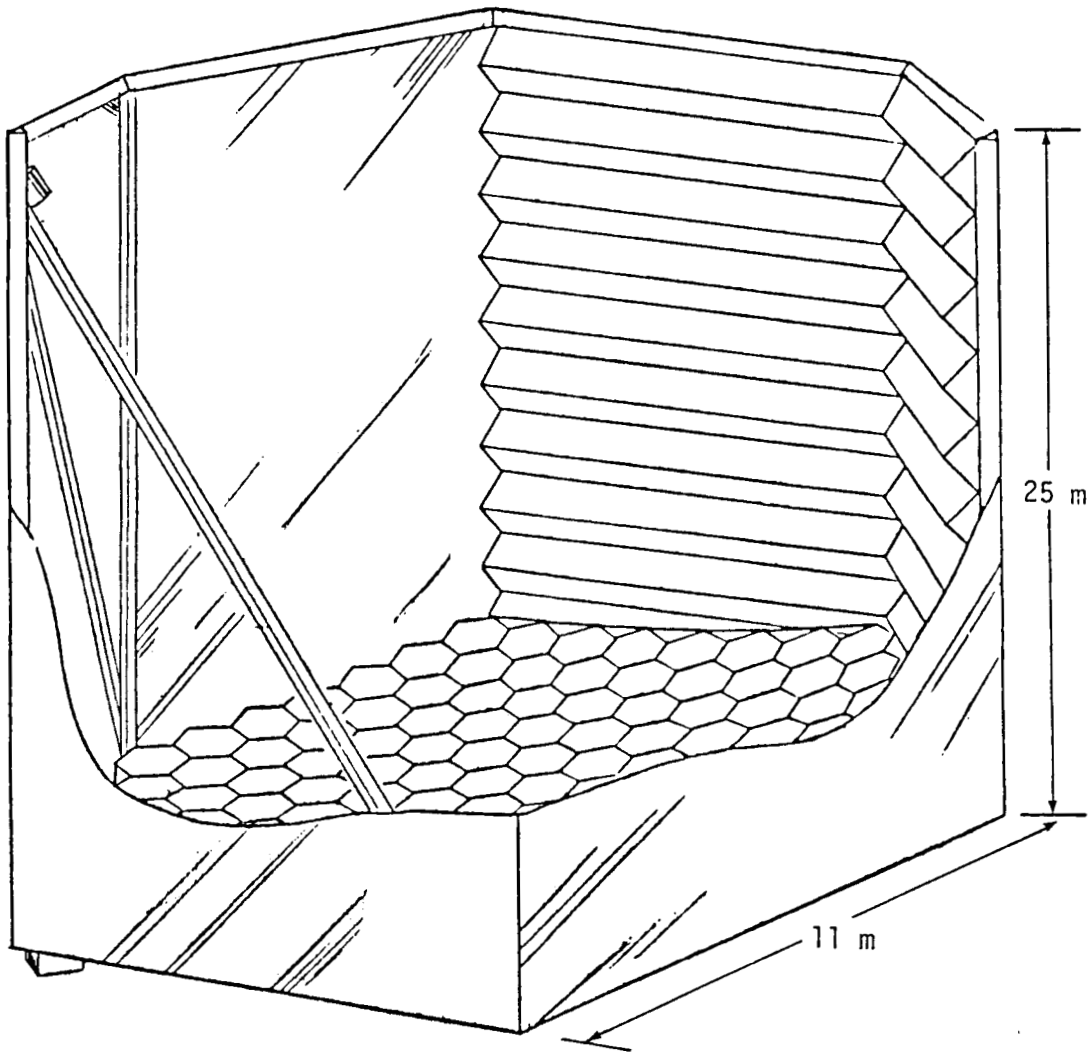

Figure 3. Reflector with thermal shielding. *036A*

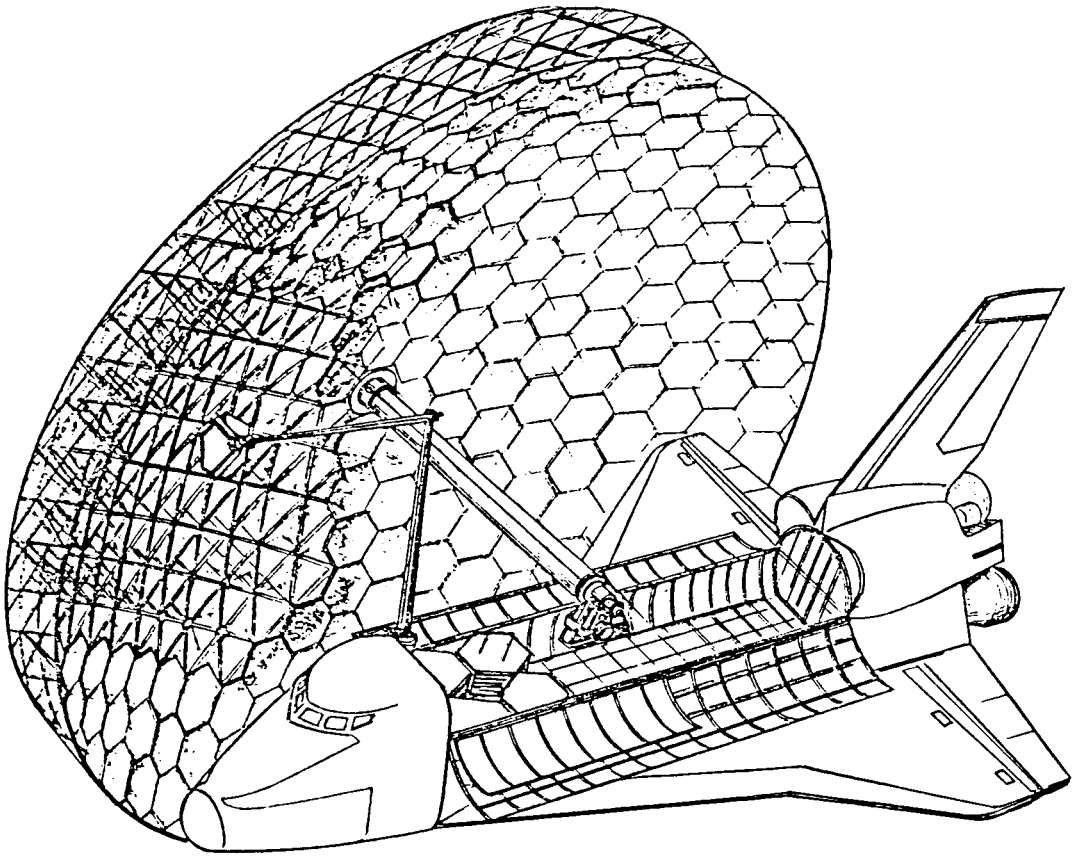

Figure 4. Mosaic reflector of spherical segments assembled by RMS from Shuttle. *008A*

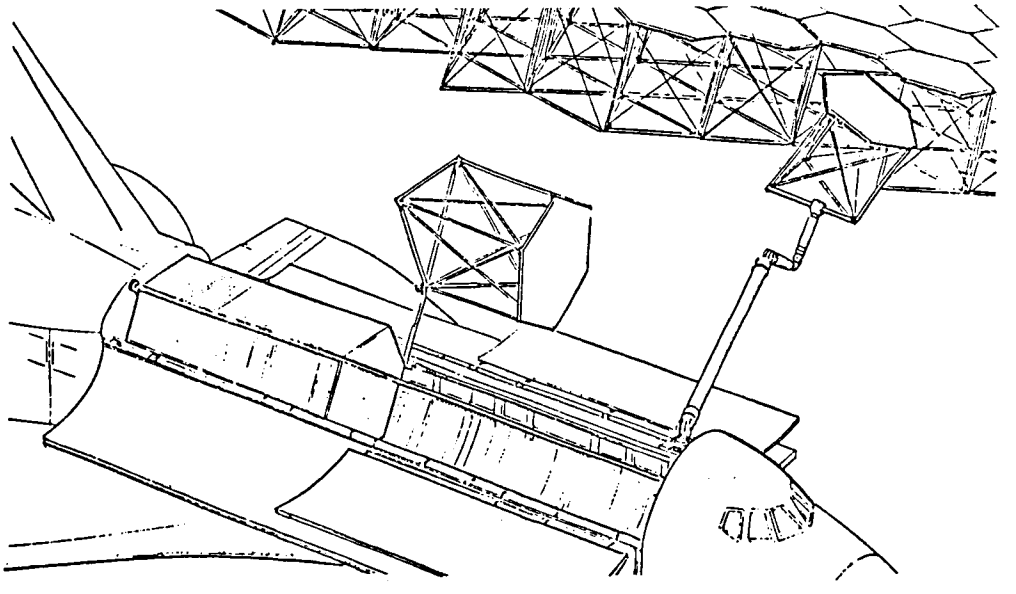

Figure 5. Astrocell.

030A

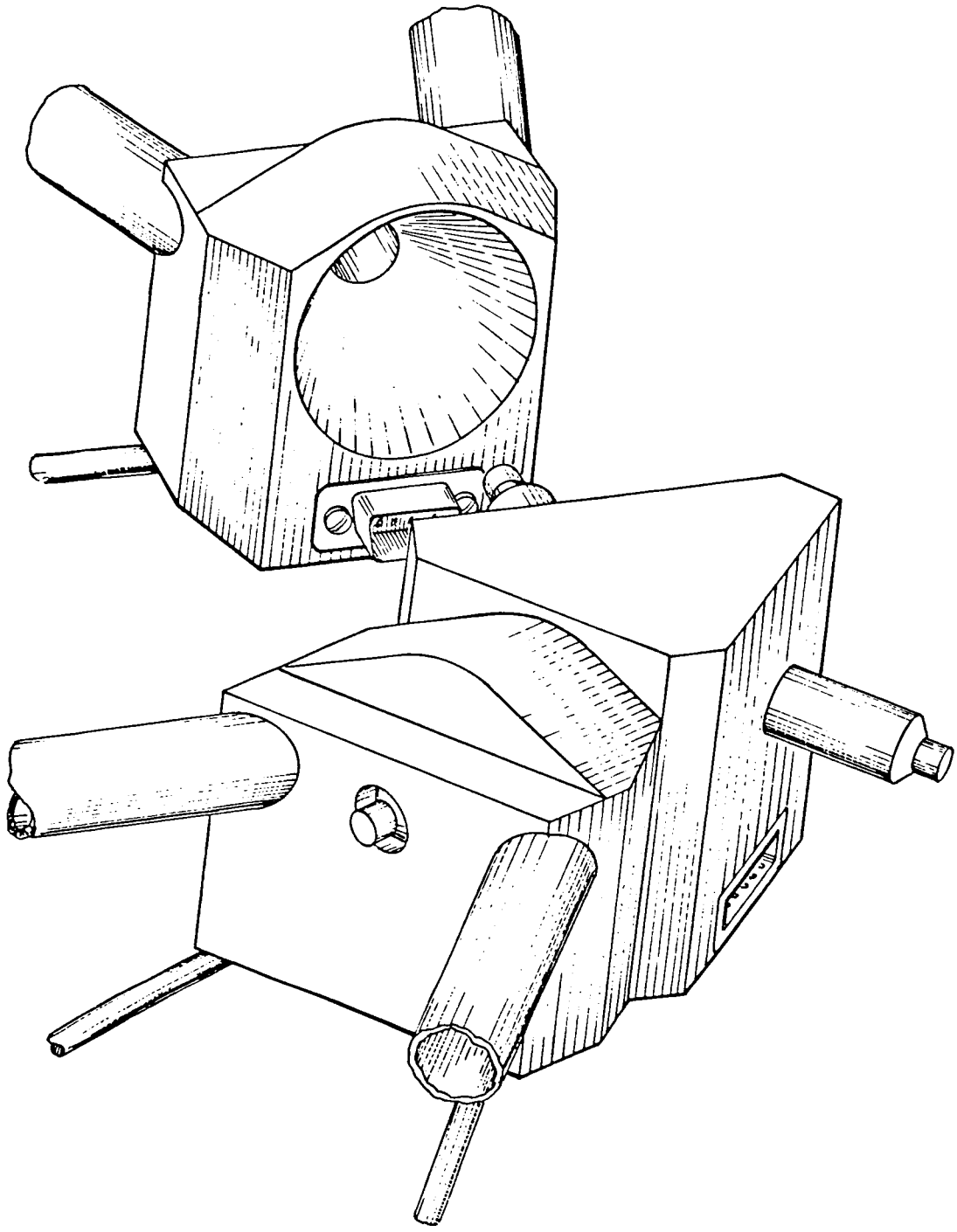

Figure 6. Typical structural/electrical joint. *011A*

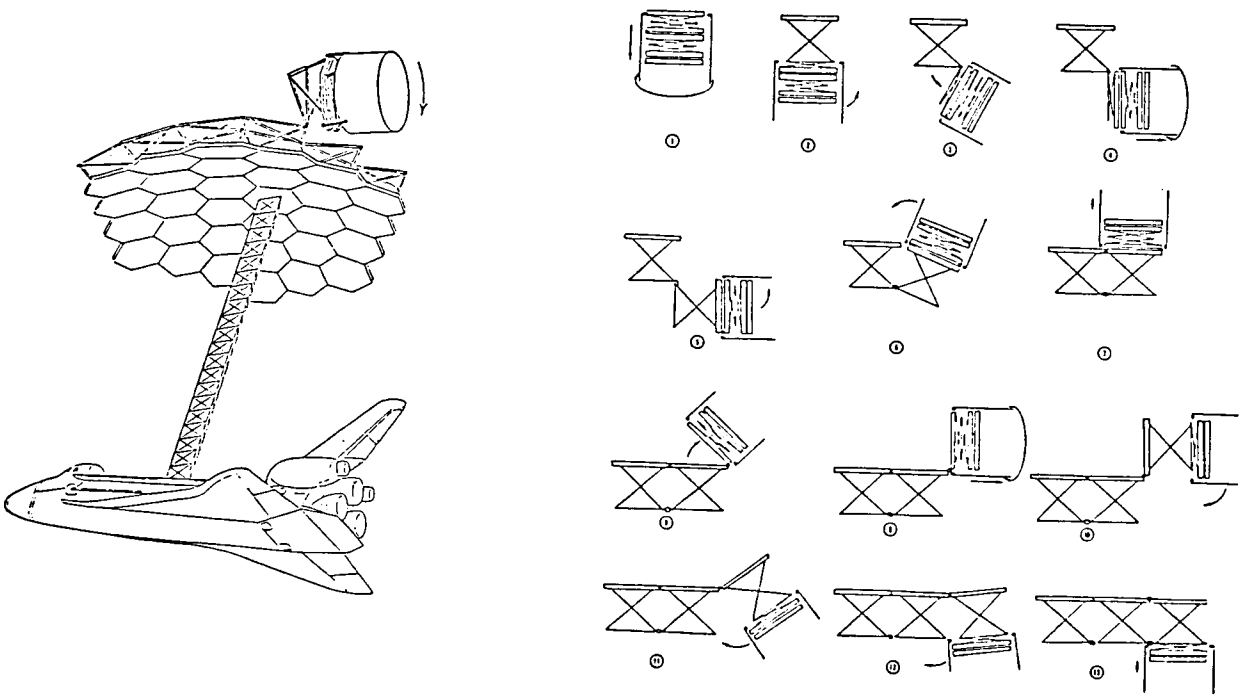

Figure 7. Sequentially deployable precision reflector. *037A*

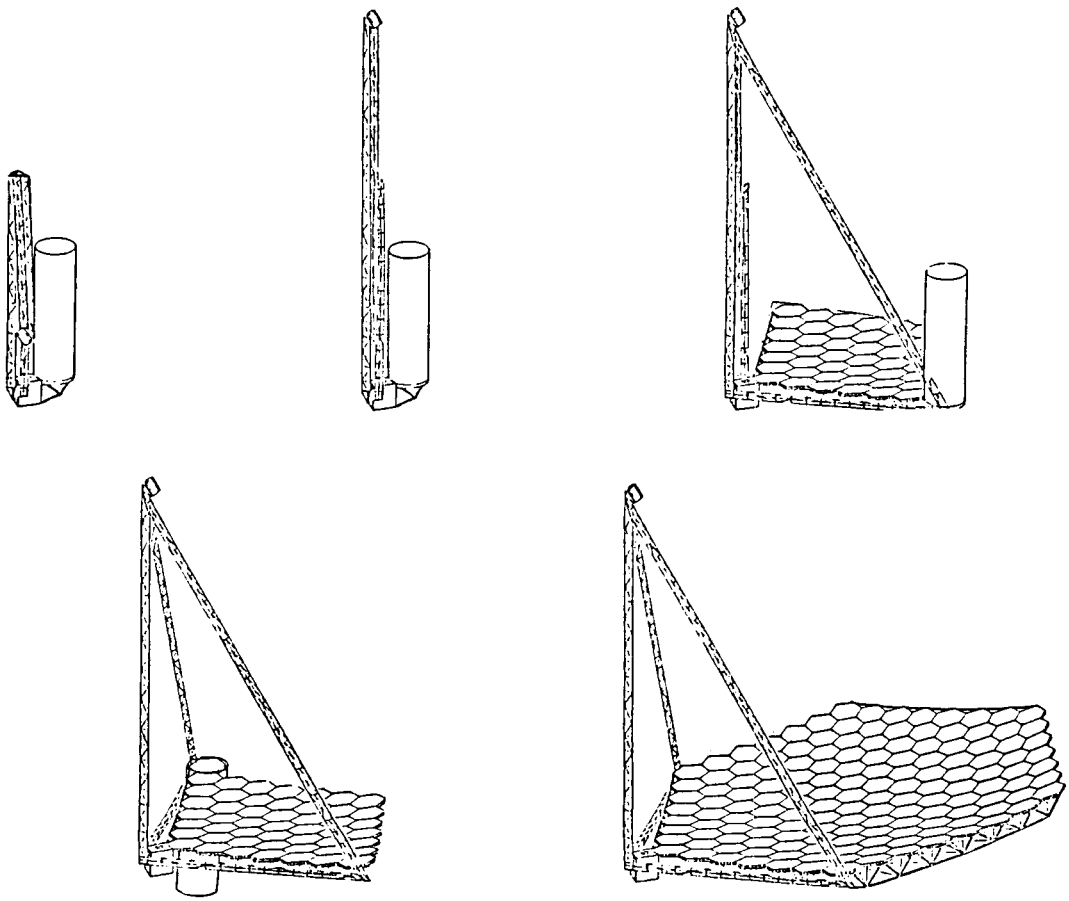

Figure 8. LDR deployment sequence. *038A*

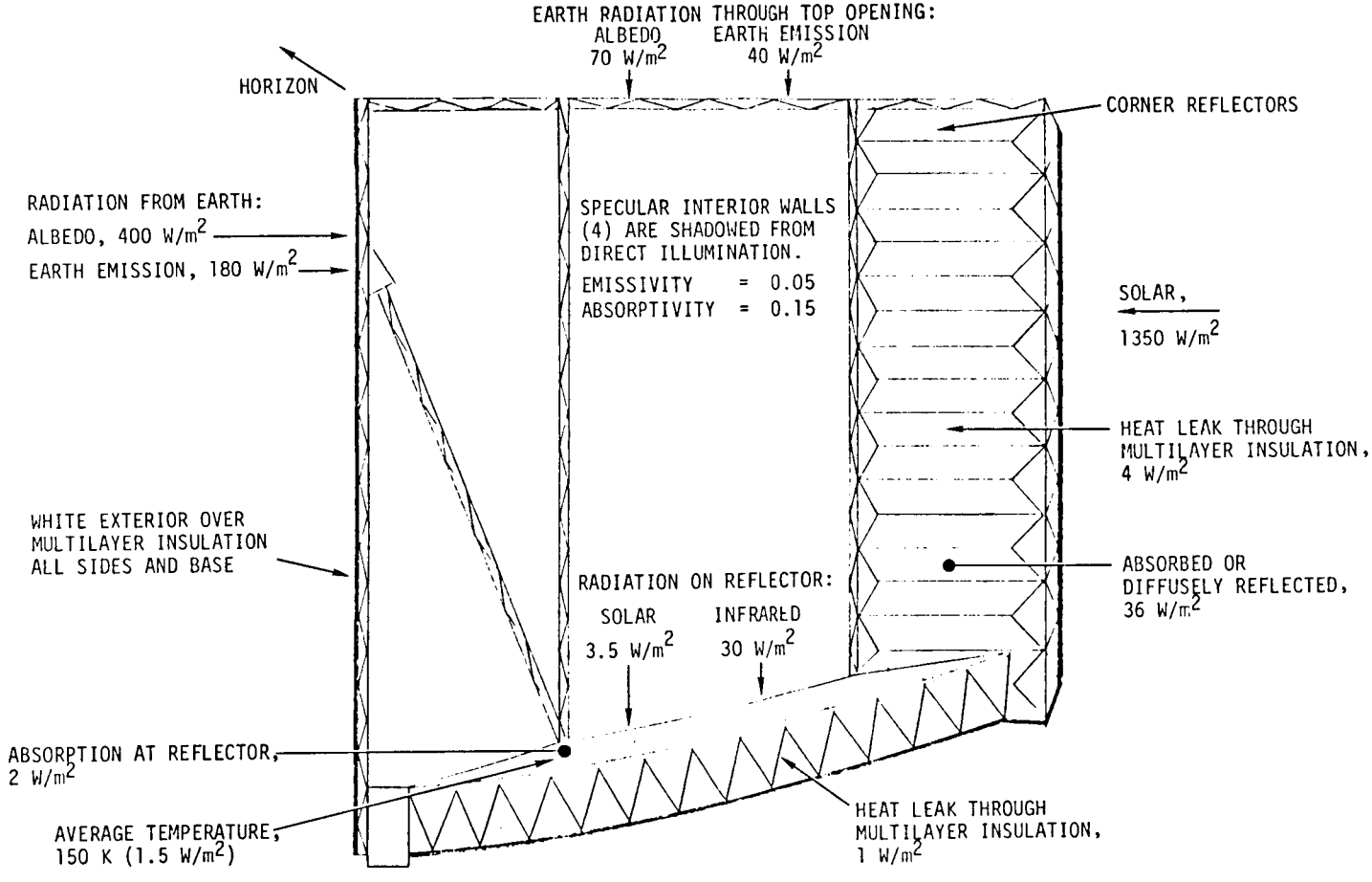

Figure 9. Thermal control.

039A

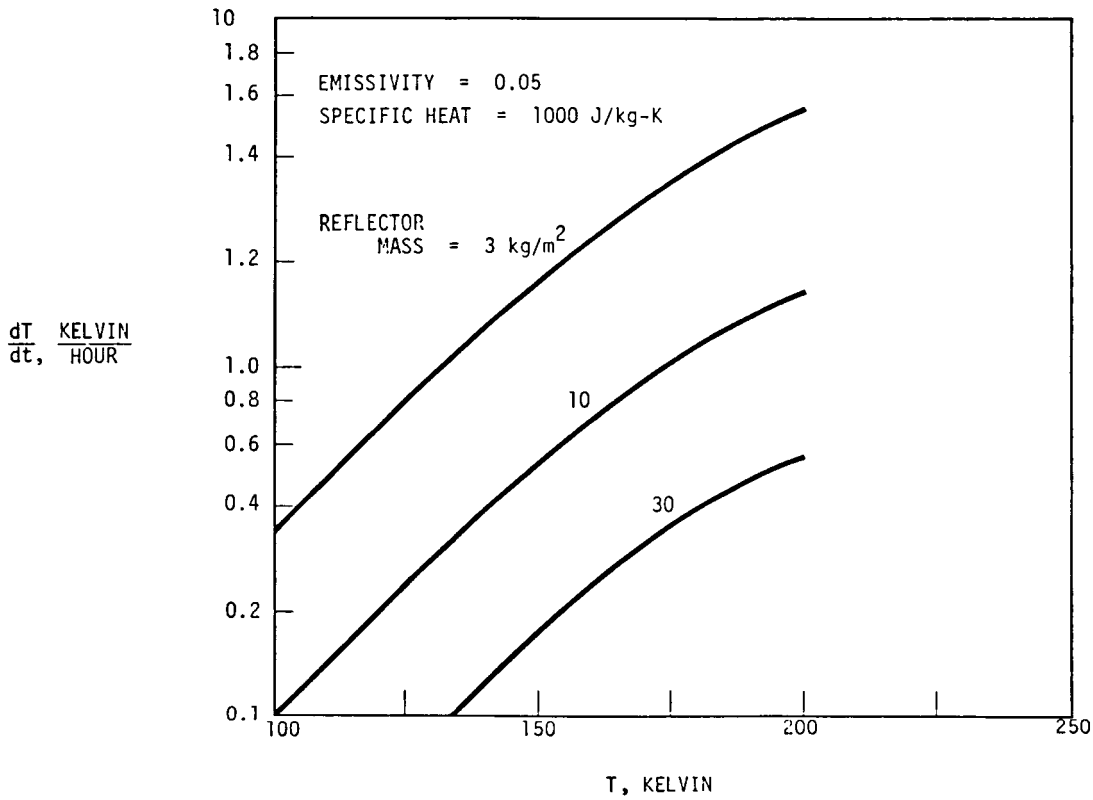

Figure 10. Transient cooling rates of reflector. *040A*

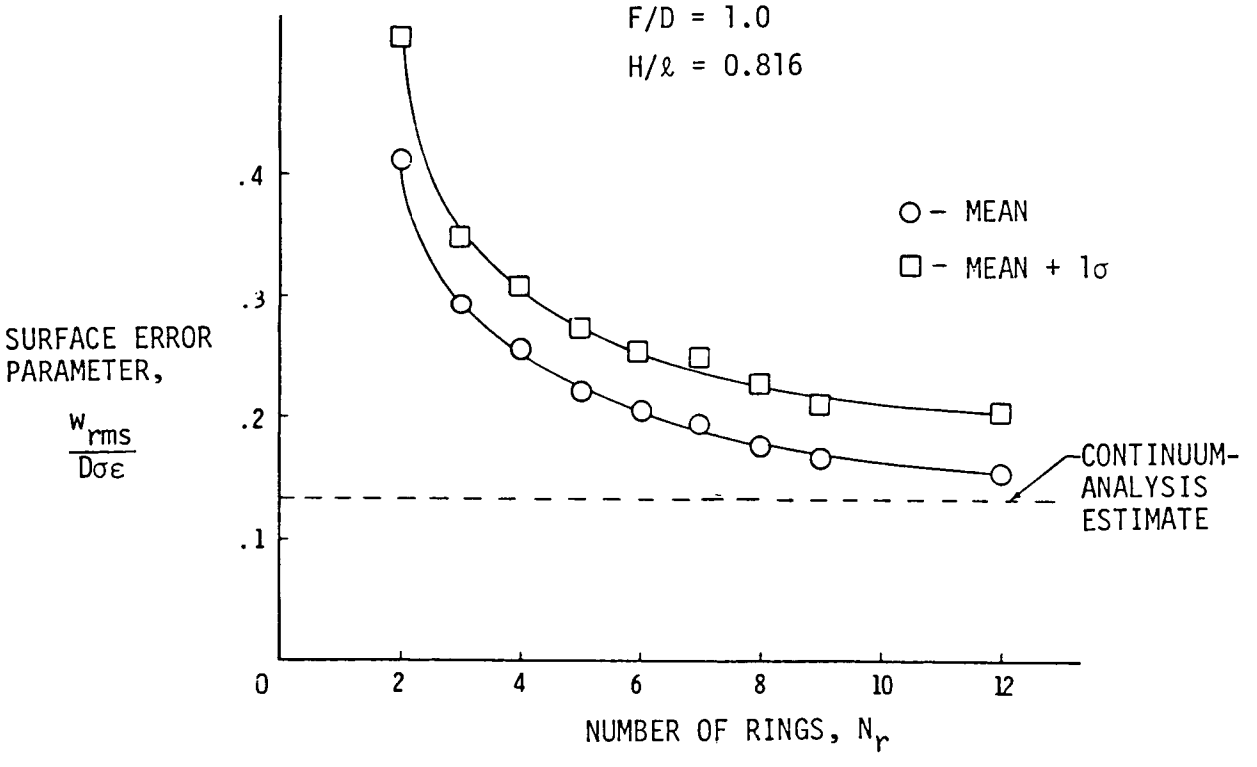

Figure 11. Surface error of a tetrahedral truss antenna. *041A*

$$\frac{\sqrt{\langle w^2 \rangle}}{D\sigma_\varepsilon} = 0.245$$

(AVERAGE STRUCTURE)

$$\frac{\sqrt{\langle w^2 \rangle + 3\sigma}}{D\sigma_\varepsilon} = 0.385$$

(WORST-CASE STRUCTURE)

NOTE: FOR $D = 20$ m, $\sigma_\varepsilon = 5 \times 10^{-5}$

THEN $D\sigma_\varepsilon = 1$ mm

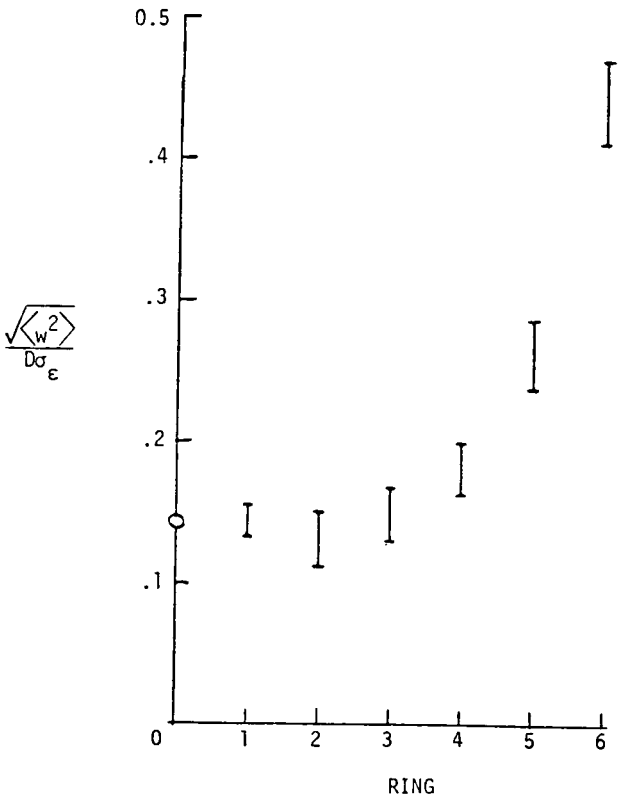

Figure 12. Fabrication-tolerance induced errors for six-ring LDR.

042A

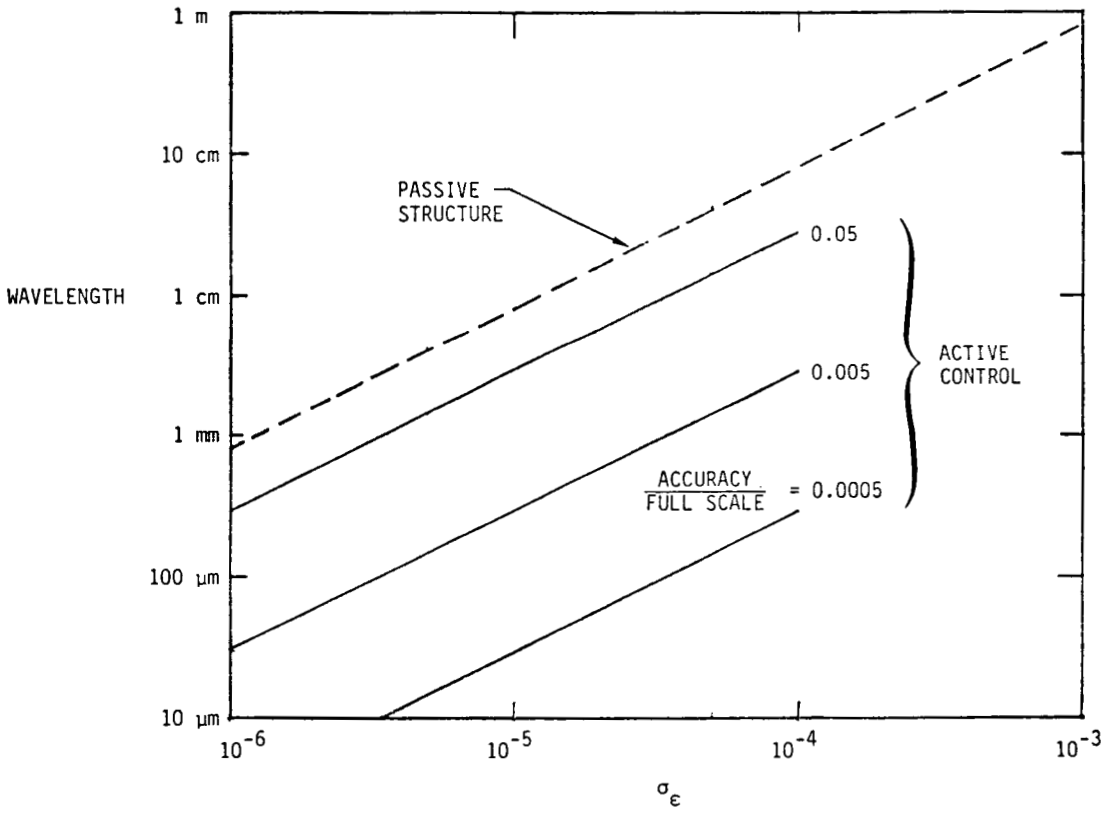

Figure 13. Limitations due to fabrication errors for baseline LDR (allowable error = wavelength/100). *043A*

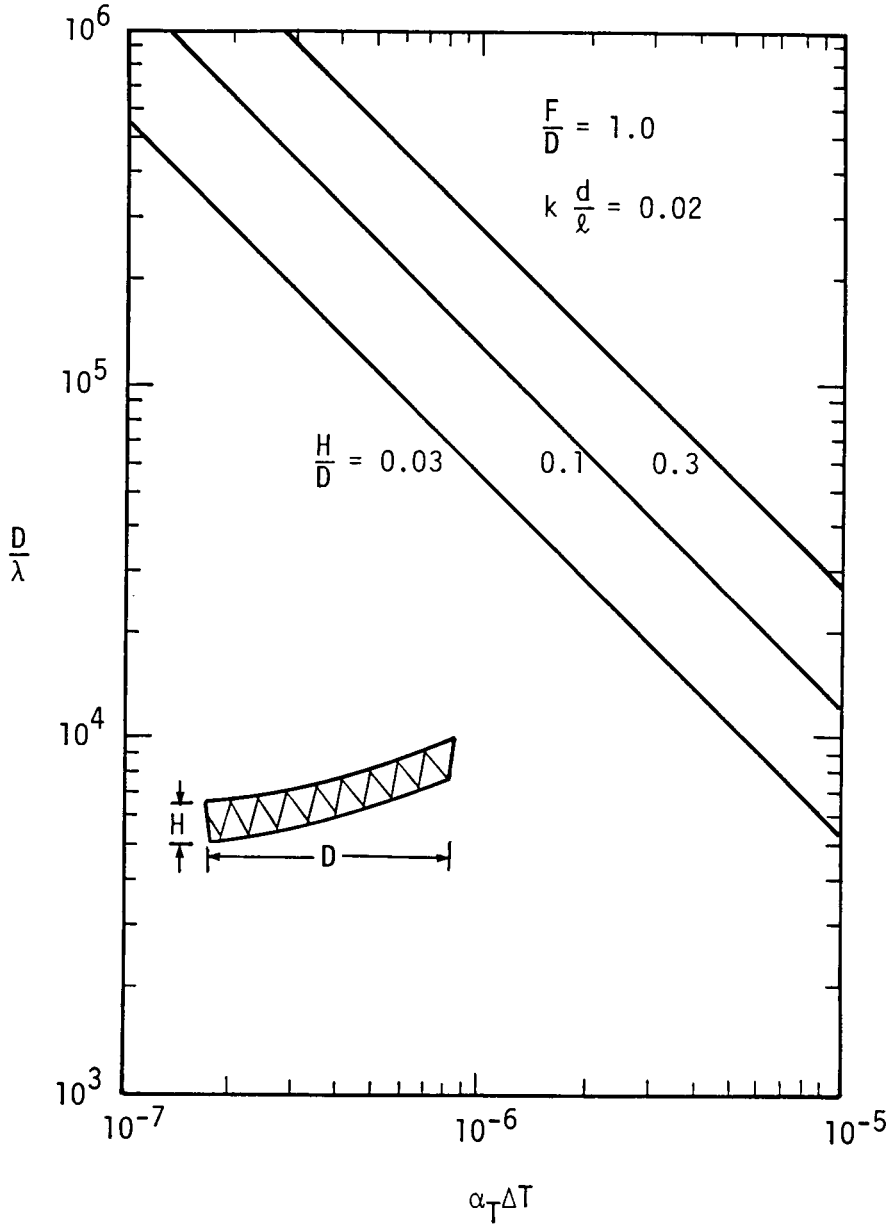

Figure 14. Limitations of the ratio of diameter to wavelength for a temperature differential of ΔT across the cavity enclosing the reflector support structure. Allowable rms surface error = $\lambda/100$ *044A*

APPENDIX

DEFORMATIONS OF A CIRCULAR ANTENNA DUE TO STATIC LOAD AT THE RIM

Let the edge of a plate-like antenna be loaded normal to its surface at the rim. Let the coordinates of a general point on the antenna of diameter D be the radius r (r less than D/2) and the angle θ. Assume the loading is symmetric about $\theta = 0$. Then, the rim loading can be written as

$$F(\theta) = \sum_{n=0}^{\infty} F_n \cos n\theta \tag{A1}$$

The loading components F_0 and F_1 will cause the antenna to accelerate as a rigid body with a consequent d'Alembert inertia loading distributed over the antenna surface of

$$p = -\left(\frac{4F_0}{D} + \frac{16F_1}{D^2} r \cos \theta\right) \tag{A2}$$

Assume that the antenna behaves structurally as a plate with stiffness D_s. Then, the equilibrium equation for the deflection w is

$$D_s \nabla^4 w = p \tag{A3}$$

At the rim, the moment must be zero and the Kirchoff shear must be F. Therefore, at r = D/2

$$\left.\begin{aligned} w_{rr} + \nu\left(\frac{1}{r} w_r + \frac{1}{r^2} w_{\theta\theta}\right) &= 0 \\ \frac{\partial}{\partial r}(\nabla^2 w) + \frac{(1-\nu)}{r}\frac{\partial}{\partial r}\left(\frac{1}{r} w_{\theta\theta}\right) &= -\frac{F}{D_s} \end{aligned}\right\} \tag{A4}$$

In order to solve the equations, let

$$w = \sum_{n=0}^{\infty} W_n(r) \cos n\theta \tag{A5}$$

substitute into Eqs. (A3) and (A4) and equate coefficients of cos $n\theta$. This gives

$$\left.\begin{aligned} \nabla_n^4 W_n &= -\frac{4F_0}{D_s D} \quad , n=0 \\ &= -\frac{16F_1}{D_s D^2} r \quad , n=1 \\ &= 0 \quad , n \geq 2 \end{aligned}\right\} \tag{A6}$$

with boundary conditions at r = D/2

$$\left.\begin{aligned} \nabla_n^2 W_n - (1-\nu)\left(\frac{1}{r}\frac{dW_n}{dr} - \frac{n^2}{r^2} W_n\right) &= 0 \\ \frac{d}{dr}\left(\nabla_n^2 W_n\right) - \frac{n^2(1-\nu)}{r}\frac{d}{dr}\left(\frac{W_n}{r}\right) &= -\frac{F_n}{D_s} \end{aligned}\right\} \qquad \text{(A7)}$$

where

$$\nabla_n^2 = \frac{d^2}{dr^2} + \frac{1}{r}\frac{d}{dr} - \frac{n^2}{r^2} \qquad \text{(A8)}$$

The general solutions of Eq. (A6), finite at the origin, are

$$\left.\begin{aligned} W_0 &= A_0 + B_0 r^2 - \frac{F_0}{16 D_s D} r^4 \\ W_1 &= A_1 r + B_1 r^3 - \frac{F_1}{12 D_s D^2} r^5 \\ W_n &= A_n r^n + B_n r^{n+2} \quad , \; n \geq 2 \end{aligned}\right\} \qquad \text{(A9)}$$

Applying the boundary conditions enables the determination of A_n for $n \geq 2$ and B_n for all n. The coefficients A_0 and A_1 represent rigid-body displacement. They are chosen so that the total average displacement and rotation are zero. Thus,

$$A_0 = \frac{B_0 D^2}{8} + \frac{F_0}{48 D_s D}\left(\frac{D}{2}\right)^4$$

$$A_1 = -\frac{2}{3} B_1 \left(\frac{D}{2}\right)^2 + \frac{F_1}{24 D_s D^2}\left(\frac{D}{2}\right)^4 \qquad \text{(A10)}$$

Carrying out the indicated substitutions yields

$$\frac{W_0}{D} = \frac{F_0 D^2}{256 D_s}\left[-\frac{2}{3}\frac{4+\nu}{1+\nu} + 2\frac{3+\nu}{1+\nu}\left(\frac{2r}{D}\right)^2 - \left(\frac{2r}{D}\right)^4\right] \qquad \text{(A11)}$$

$$\frac{W_1}{D} = \frac{F_1 D^2}{384 D_s}\left[-\frac{31+5\nu}{6(3+\nu)} + \frac{2(5+\nu)}{3+\nu}\left(\frac{2r}{D}\right)^2 - \left(\frac{2r}{D}\right)^4\right]\left(\frac{2r}{D}\right) \qquad \text{(A12)}$$

$$\frac{W_n}{D} = \frac{F_n D^2}{16 n (n^2-1) D_s}\left\{\frac{(n+1)\,4 + (n-2)(1-\nu)}{n(1-\nu)(3+\nu)} - \frac{n-1}{3+\nu}\left(\frac{2r}{D}\right)^2\right\}\left(\frac{2r}{D}\right)^n, \quad n \geq 2 \qquad \text{(A13)}$$

Of primary interest is the value of the mean-square displacement.

$$\overline{w^2} = \frac{4}{\pi D^2}\int_0^{D/2}\int_0^{2\pi} w^2 r\,dr\,d\theta \qquad \text{(A14)}$$

Substituting from Eq. (A5) yields

$$\overline{w^2} = \overline{W_0^2} + \frac{1}{2}\sum_{n=1}^{\infty} W_n^2 \tag{A15}$$

where

$$\overline{W_n^2} = 2\int_0^1 W_n^2\left(\frac{D}{2}\rho\right)\rho d\rho \tag{A16}$$

is the mean-squared value of W_n and $\rho = 2r/D$.

Nondimensionalize with respect to the diameter D.

$$\frac{\overline{w^2}}{D^2} = \overline{\left(\frac{W_0}{D}\right)^2} + \frac{1}{2}\sum_{n=1}^{\infty}\overline{\left(\frac{W_n}{D}\right)^2} \tag{A17}$$

Substitute from Eqs. (A11) to (A13) to give, for $\nu = 1/3$

$$\overline{\left(\frac{W_0}{D}\right)^2} = 2.043 \times 10^{-5}\left(\frac{F_0 D^2}{D_s}\right)^2 \tag{A18}$$

$$\overline{\left(\frac{W_1}{D}\right)^2} = 7.648 \times 10^{-7}\left(\frac{F_1 D^2}{D_s}\right)^2 \tag{A19}$$

$$\overline{\left(\frac{W_n}{D}\right)^2} = \frac{1.7578n^3 + 7.2422n^2 + 8.7188n + 3.3750}{n^4(n-1)^2(n+1)^2(n+2)(n+3)} \times 10^{-2}\left(\frac{F_n D^2}{D_s}\right)^2 , \quad n \geq 2 \tag{A20}$$

As an example, consider the case where the edge loadings are concentrated loads at $\theta = 0$ and $\pm\alpha$ which balance each other and produce a moment of Q. The loads are

$$\left.\begin{aligned} P(0) &= \frac{2Q}{D(1-\cos\alpha)} \\ P(\pm\alpha) &= -\frac{Q}{D(1-\cos\alpha)} \end{aligned}\right\} \tag{A21}$$

Thus, for this case

$$\left.\begin{aligned} F_0 &= 0 \\ F_n &= \frac{4}{\pi}\frac{Q}{D^2}\frac{1-\cos n\alpha}{1-\cos\alpha} \end{aligned}\right\} \tag{A22}$$

The series of Eq. (A17) has been evaluated by keeping enough terms to achieve convergence. The results are given in the following table where

$$w_{rms} = \sqrt{\overline{w^2}} \tag{A23}$$

RMS DEFORMATIONS FOR EDGE-LOADED DISK

ALPHA,°	RMS DEFORMATION, $\frac{w_{rms}/D}{Q/D_s}$
10	6.214×10^{-2}
20	5.922
30	5.548
40	5.122
50	4.660
60	4.177
70	3.683
80	3.187
90	2.697
100	2.221
110	1.768
120	1.347
130	0.968
140	.646
150	.404
160	.281
170	.274
180	.287

1. Report No.	2. Government Accession No.	3. Recipient's Catalog No.
NASA CR-3800		

4. Title and Subtitle	5. Report Date
SUPPORT STRUCTURES FOR LARGE INFRARED TELESCOPES	July 1984
	6. Performing Organization Code

7. Author(s)	8. Performing Organization Report No.
John M. Hedgepeth	ARC-TN-1121
	10. Work Unit No.

9. Performing Organization Name and Address		11. Contract or Grant No.
Lockheed Missiles & Space Co., Inc. P. O. Box 504 Sunnyvale, CA 94086	Subcontractor: Astro Research Corp. 6390 Cindy Lane Carpinteria, CA 93013	NAS1-16923
		13. Type of Report and Period Covered
12. Sponsoring Agency Name and Address		Contractor Report
National Aeronautics and Space Administration Washington, DC 20546		14. Sponsoring Agency Code 506-53-43-01

15. Supplementary Notes

John M. Hedgepeth: Astro Research Corporation, Carpinteria, California.
Langley Technical Monitor: Harold G. Bush
Prepared under Subcontract EG50C7150M.

16. Abstract

An infrared telescope requires an accuracy of its reflecting surfaces of less than a micrometer. Future missions may require such accuracy from telescopes that are 20 meters or larger in diameter. The structure for supporting such a telescope will most probably take the form of a deep truss. Various approaches for constructing the primary mirror in space are illustrated. One that employs automated deployment of interconnected reflector-structure modules is described in detail. Estimates are made of the precision obtainable with properly configured truss structures and the required ability of active control systems for achieving the desired accuracy.

17. Key Words (Suggested by Author(s))	18. Distribution Statement
Deployable Structures Space Structures Surface Accuracy Antennas Vibrations Telescopes	Unclassified - Unlimited Subject Category 39

19. Security Classif. (of this report)	20. Security Classif. (of this page)	21. No. of Pages	22. Price
Unclassified	Unclassified	49	A04

For sale by the National Technical Information Service, Springfield, Virginia 22161

NASA-Langley, 1984